UCLA
COMPUTATIONAL AND APPLIED MATHEMATICS

Quantum Wave Turbulence

M.B. Haeri
S.J. Putterman
A. Garcia
P. H. Roberts

October 1991

CAM Report 91-24

Department of Mathematics
University of California, Los Angeles
Los Angeles, CA. 90024-1555

QUANTUM WAVE TURBULENCE

M.B. Haeri, S.J. Putterman,

Department of Physics, University of California, Los Angeles, CA 90024, USA

A. Garcia,

Department of Physics, San Jose State University, CA 95192, USA

and

P.H. Roberts

Department of Mathematics, University of California, Los Angeles, CA 90024, USA

ABSTRACT

The nonlinear quantum kinetic equation for the interaction of sound waves is solved via analytic and numerical techniques. In the classical regime energy cascades to higher frequency (ω) according to the steady state power law $\omega^{-3/2}$. In the quantum limit, the system prefers a reverse cascade of energy which follows the power law ω^{-6}. Above a critical flux, a new type of spectrum appears which is neither self-similar nor close to equilibrium. This state of nonlinear quantum wave turbulence represents a flow of energy directly from the classical source to the quantum degrees of freedom.

The anharmonic terms in the Hamiltonian for fluid mechanics account for the scattering of one sound wave by another. In the classical limit this nonlinear effect is referred to as the wave-wave interaction.[1] In the quantum limit the corresponding phenomenon is called the phonon-phonon interaction.[2] For a fluid [3] and even more complex systems [4] the quantum and classical regimes can be bridged by a single kinetic equation. This equation describes the nonlinear time development of the spectral intensity along with effects that are due to the scattering of acoustic energy by the zero point motion .[5]

We have used this kinetic equation to study the fate of acoustic energy that is injected into a fluid so as to drive it far off equilibrium (i.e. far from the Planck distribution). In the classical region of wave-number space, energy cascades from low frequency to higher frequency so as to generate a steady state power law distribution [6] that is analogous to the Kolmogorov spectrum [7] of vortex turbulence. This distribution for classical wave turbulence is shown in figure 1. Classical wave turbulence accounts for the spectrum of wind driven surface waves in the ocean [8] and Alfvèn waves driven by the solar wind.[9] In the quantum region of parameter space there is a reverse cascade of energy from higher to lower wave numbers. As shown in Figure 2, the steady state of quantum wave turbulence is also characterized by a power law dependence for the spectral intensity. We believe that this reverse quantum cascade underlies the high frequency phonon redistribution processes measured in references [10, 11].

When the input of low frequency energy exceeds a critical value, we find that it is possible to realize a cascade in which energy is mechanically transported directly from the classical to the quantum domain. An example of this new off-equilibrium steady state, which spans the classical and quantum domains, is shown in Figure 3.

To study turbulence in quantum systems we consider a "sea" of interacting dispersionless waves with small interactions between waves. For this case, the frequency ω is related to the wavenumber k by the expression $\omega = ck$, where c is the speed of the sound. The lack of dispersion for acoustic waves implies a basic 3-wave resonant nonlinear interaction such that

waves with frequencies ω_1 and ω_2 scatter to produce waves with frequency $\omega_3=\omega_1 \pm \omega_2$. A nonlinear Boltzmann type of equation describes the time rate of change of the wave action due to three-wave interactions. The general kinetic equation valid in both the classical and quantum limits is [2, 3, 5]

$$\frac{\partial I(\omega_n)}{\partial t} = \frac{2\pi^3 G^2 c}{\rho V^2}\left\{\int_0^{\omega_n}\left[I(\omega_n-\omega_k)I(\omega_k) - I(\omega_n)\left(I(\omega_k)+I(\omega_n-\omega_k)+\hbar\right)\right]\right.$$

$$\times \quad \sigma(\omega_n-\omega_k)\,\sigma(\omega_k)\,d\omega_k$$

$$\left. +2\int_0^{\infty}\left[I(\omega_n+\omega_k)\left(I(\omega_k)+I(\omega_n)+\hbar\right) - I(\omega_k)\,I(\omega_n)\right]\sigma(\omega_n+\omega_k)\,\sigma(\omega_k)\,d\omega_k\right\} \tag{1}$$

where $\sigma(\omega)=V\omega^2/2\pi^2c^3$ corresponds to the density of states, V is the container volume, "I" is the mean averaged action, ρ is the density, $G = 1 + (\rho/c)dc/d\rho$ is the Gruneisen coefficient, and $\hbar$ is Planck's constant. The coupling between different modes is determined by G. The kinetic Equation (1) has all of the information of the quantum theory of interacting phonons. The energy per unit volume per unit frequency interval, or so called spectral intensity can be obtained from $e(\omega)=I(\omega)\omega\sigma(\omega)/V$.

The equilibrium solution to Equation (1) is the Planck spectrum:

$$I(\omega) = \frac{\hbar}{e^{\hbar\omega/k_BT} - 1} \tag{2}$$

where k_B is Boltzmann's constant and T is the temperature. For small $\hbar$; $e(\omega) \rightarrow k_BT\omega^2/2\pi^2c^3$ which is equipartition of energy. For $\hbar\omega/k_BT >>1$; $I \rightarrow \hbar\exp(-\hbar\omega/k_BT)$ which is Wien's law.

The analytic solutions for wave turbulence follow from the conservation of wave energy with respect to its flow in phase space: [6]

$$\frac{\partial e(\omega_n)}{\partial t} + \frac{\partial q(\omega_n)}{\partial \omega_n} = 0 \tag{3}$$

where $q(\omega)$ is the energy throughput (erg/cm^3 sec). In the steady state $q=q_o$ is a constant; using this fact (3) yields:

$$q_o = -\frac{1}{2\pi^2 c^3}\int \omega_n^3 \frac{\partial I(\omega_n)}{\partial t}\, d\omega_n \tag{4}$$

where by $\partial I(\omega_n)/\partial t$ we mean the expression on the right hand side of (1). The classical limit of (4) involves the quadratic terms in "I" which clearly balance when "I" is proportional to $\omega^{-9/2}$. The strong quantum limit of (4) involves the linear terms in (1) and these balance for "I" proportional to ω^{-9}. Substituting these forms for the solution into (4), one recovers the well known power spectrum for classical wave turbulence: [6]

$$e(\omega) = \frac{A\left(\rho c^2 q_o\right)^{1/2}}{\sqrt{\pi}\,|G|\,\omega^{3/2}} \tag{5}$$

as well as the quantum power spectrum of off-equilibrium noise:

$$e(\omega) = \frac{a_o 2\pi q_o c^5 \rho}{\hbar G^2 \omega^6}. \tag{6}$$

In (5) the constant $A \approx 1/(52.42)^{1/2} \approx 0.138$ [see reference 12] and in (6) the constant $a_o = 1800/37$. These solutions apply in the steady state and when $e(\omega)$ is large compared with its value in equilibrium. Generalizations of (5) which account for different dimensions and dispersion laws lead to explanations for wind driven surface wave spectra.[8]

The quantum solution decays more slowly than the Planck spectrum; therefore, in contrast with the classical cascade, we are dealing here with a reverse cascade of energy from a high

frequency to a low frequency. The reverse cascade of energy in the strong quantum limit is evidence for spontaneous decay of phonons or frequency down-conversion. [10, 11, 13]

We now turn to the numerical solution of Equation (1). These solutions are of value in 1) verifying the validity of the steady state cascades (5) and (6), 2) elucidating the temporal development of the classical and quantum off-equilibrium spectra, and 3) determining the spectrum of wave turbulence at the interface of classical and quantum mechanics. Numerical solutions of the strictly classical kinetic equation have been carried out to verify the exponent in the classical steady state spectrum.[14, 15]

The nonlinear coupling of the classical and quantum domains (case 3) can be appreciated by comparing equation (5) and equation (2). In particular, if the low frequency input flux (q_o) is chosen to be larger than a critical flux q_c, then the distribution (5) goes over the top of the spectrum where the equilibrium energy is a maximum (and the frequency is $\omega_p = 2.88 k_B T/\hbar$). The critical flux is that value of q at which (5) is tangent to the Planck spectrum or

$$q_c = A_o \frac{G^2 (k_B T)^9}{\rho c^8 \hbar^7} \tag{7}$$

where "A_o" is a constant. For this range of parameters the motion is both quantum and nonlinear. Similar comments apply to the reverse flux spectrum (6). Indeed, the value of q at which the spectrum (6) is tangent to the Planck law is also given by (7) but with a different value of the proportionality constant.

The continuous kinetic equation was discretized by solving for the action at N uniformly spaced frequencies, with grid spacing Δ, and by using a trapezoidal rule to evaluate the integrals on the right of (1). One merit of the method of discretization is that the equilibrium solution of (8) is again the Planck spectrum (2). In addition, a source for injecting energy and a sink for removing energy were added to equation (1) to obtain:

$$\frac{\partial I_i}{\partial t} = \sum_{j=1}^{i-1} j^2 (i-j)^2 \{ I_j I_{i-j} - I_i (I_{i-j} + I_j + 1) \}$$

$$+ 2 \sum_{j=1}^{N-i} j^2 (i+j)^2 \{ I_{i+j} (I_i + I_j + 1) - I_i I_j \}$$

$$+ q_o k_o^{-3} \delta_{i,k_o} - q_s k_s^{-3} \delta_{i,k_s} . \qquad (8)$$

In order to obtain (8) we introduced the dimensionless time, temperature, flux, action, and spectral density

$$\bar{t} = \frac{t G^2 \Delta^5 I}{2\pi c^5 \rho}; \qquad \bar{T} = \frac{k_B T}{\hbar \Delta}$$

$$\bar{q} = \frac{q 4\pi^3 c^8 \rho}{G^2 \Delta^9 I^2}; \quad \bar{I} = \frac{I}{I}; \quad \bar{e}_j = j^3 \bar{I}_j \qquad (9)$$

where the characteristic action "I" is $k_B T/N\Delta$ in the classical limit ($\bar{T}/N > 1$) and $I = \hbar$ in the quantum limit $\bar{T}/N << 1$ (in equation 8 we have displayed the case $I = \hbar$). The mode numbers for the source and sink have been denoted by k_o and k_s, and $\bar{\omega} = \omega/\Delta$. In discretizing (1), ω_j is replaced by Δj and $I_j = I(j\Delta)$. In expression (8) and in the figures the bars have been dropped. In expression (8) the energy flux is supplied to just one mode and similarly removed. However, as we demonstrate later, energy can be supplied and removed over a distribution of modes as long as the input energy is equal to the output energy when a steady state is achieved. In references 12 and 13 the removal of energy was accomplished with dissipative terms.

Expression (8) was implemented on an Alliant FX-80 and solved for N=1,000. The equilibrium Planck distribution was used as the initial condition. The initial bath temperature T was controlled to access the classical, strong quantum, and the nonlinear quantum regimes. Here, the classical region is defined as that region where in equilibrium all 1000 modes follow a Rayleigh-Jeans type of distribution; in the strong quantum regime most of the 1000 modes follow Wein's Law in equilibrium; in the non-linear quantum regime neither of the two aforementioned distributions holds true, a Planck distribution must be used in the equilibrium case.

Figure 1 depicts the time evolution of the classical spectrum from a Rayleigh-Jeans distribution to a steady state spectral energy distribution following a -3/2 power law in the inertial regime. Figure 1 is a log-log plot of the energy per unit volume per unit frequency as a function of frequency for 9 different time steps starting from t=0 to $t=10^{-12}$ where a steady-state is achieved. An initial bath temperature of 2000 was selected to access the classical regime across all 1000 modes. A flux of 10^{24} was supplied over a Gaussian distribution of modes centered at $\omega=3$ and subsequently removed over modes greater than 300 in such a manner so as to preserve the initial temperature of the Rayleigh-Jeans distribution at high frequencies. This is accomplished by increasing the output flux q_s in (8) (starting with $q_s = 0$ at $t = 0$) after each time step until a steady state is achieved in which $q_o = q_s$. Energy was injected over a Gaussian distribution of modes so as to couple the energy smoothly from low to high frequencies. Supplying energy to just one mode results in a forward "hopping" of energy among the harmonics of the system. The steady-state spectrum in Figure 1 can be divided up into three regions: the region where energy is supplied or source, the inertial region, and a sink where energy is removed. The spectrum follows a -3/2 power in the inertial region between $\omega=10$ and $\omega=100$ before curving around and meeting the initial equilibrium solution. The -3/2 power law is achieved to three digits accuracy, and the Kolmogorov constant for acoustic turbulence "A" is found to be approximately 0.15. As the bath temperature is increased beyond 2000, the numerically calculated coefficient approaches the analytic value of A given in (5).

Although a forward cascade of energy is preferred in the strong classical regime, it is possible to inject energy at a high frequency and remove it from a low frequency. The maximum flux which can cascade in the reverse direction is down by a factor of 10^7 from the forward flux.

As an example of how to recover the physical variables we take $\rho = 1.$ g/cc, $c = 10^4$ cm/sec, $\Delta = 10^6$ Hz so that $T = 20.$ mK. Then a dimensionless time of order 10^{-13} corresponds to a real time of 10^4 s and flux of order 10^{24} corresponds to a Mach number of order 10^{-6}. For a real system N can be much larger, but we claim that the qualitative insights obtained here with N = 1,000 will remain valid.

The time evolution of the quantum spectrum from a Planck distribution to a steady state spectral energy distribution following a steep -6 power of the frequency is shown in Figure 2. Unlike the classical case, a reverse cascade of energy is preferred. Energy is injected and removed over a Gaussian distribution of modes centered at $\omega = 800$ and $\omega = 10$ respectively. The bath T = 1.5, and the flux is 1000. Similar to Figure 1, Figure 2 illustrates seven logarithmically spaced time-steps starting from $t=0$ and ending at $t=10^{-3}$ where a steady-state is achieved. The power law in the inertial regime, located between $\omega = 700$ and $\omega = 40$, corresponds to ω^{-6} (ω^{-9} for action I), and the numerically computed constant is the same as a_o in expression (6) to three digits. Although a reverse cascade is strongly favored, a negligible amount of energy cascades forward of the source to higher frequencies. The quadratic terms in the kinetic equation are responsible for this small forward cascade of energy.

In the nonlinear quantum regime ($q \geq q_c$) neither the linear nor quadratic terms can be neglected. This is the transitional region between classical and quantum mechanics. The spectrum in this regime is neither self-similar nor close to equilibrium. Thus, our only means of investigating the response in this region is numerical.

In this regard consider the case where energy is injected at small ω and removed at ω_p. As q is increased, the value $q = q_c \approx 60T^9$ is eventually reached. At this value the off-equilibrium spectrum follows the -3/2 power law at low ω and then turns up so as to become tangent to the Planck spectral peak as shown in Figure 4, plot A (for this plot $q = 6 \times 10^{19} \approx q_c$ and T = 100 and

energy is supplied over a Gaussian distribution centered at $\omega = 4$). It is important to mention that even if energy were removed at frequencies higher than ω_p, the steady state spectrum would have the same form (e.g. Figure 4, plot A or Figure 1) provided of course that $q \leq q_c$. Also shown in figure 4 (plot B) is the case where $q = 5 \times 10^{20} > q_c$; the dynamical spectrum following a -3/2 power law and then curves down to meet the Planck spectrum at ω_p.

Above the critical flux the steady state spectral density is dramatically altered when the sink(s) are situated above ω_p. As shown in figure 3, the classical cascade carries past the Planck maximum and then turns down with a slope steeper than Wien's law so as to meet the Planck spectrum in the quantum domain. This figure was generated for $q = 10^{17} > q_c$ and $T = 35$ where the energy is input over a Gaussian distribution of modes centered at $\omega = 3$ and removed at modes greater than 300. For $q > q_c$ a new spectrum also appears in the reverse cascade. In this case a -6 power law becomes concave downward before joining the Planck distribution as shown in Figure 5 (also indicated is the presence of a small bottleneck of energy at the high frequency source).

The physics of far off-equilibrium waves (phonons) differs from the physics of vortex flows (turbulence) in that there exits a kinetic (Boltzmann type) equation for the development of the spectral density [6]. Furthermore, this kinetic equation can be written down in a form that spans both classical and quantum mechanics. In this paper we have studied this kinetic equation and demonstrated the classical and quantum forward and reverse cascades of energy along with the dynamical approaches to the steady state spectra. Agreement between the calculated and simulated Kolmogorov constants for acoustic turbulence has been demonstrated. In addition, we have found a new spectrum at the interface of classical and quantum mechanics which represents a direct nonlinear transport of energy from the classical source to quantum sink.

ACKNOWLEDGMENTS

This research was supported by the U.S. DOE Office of Basic Energy Science Division of Engineering and Geosciences (for SJP) and by the ONR grant N00014-86-0691 (for PHR). The research of M.B.H. was supported by the Hughes Aircraft Company. We are grateful to the Mathematics department at UCLA for generous time allocations on their Alliant FX-80 machine.

REFERENCES

1. Benney, D.J. and Saffman, P.G., Proc. R. Soc. London, Ser. A **289**, 301 (1966); Newell, A.C. and Aucoin, P.J., J. Fluid Mech. **49**, 593 (1971).

2. Khalatnikov, I.M., *Introduction to the Theory of Superfluidity* , (Benjamin, New York, 1965).

3. Landau, L.D and Khalatnikov, I.M., *The theory of the viscosity of helium II: 1. Collisions of elementary excitations in helium II*, (1949), English translation in ter Haar, D., ed., Collected papers of L.D. Landau (Pergamon, Oxford, 1965), p. 494.

4. Peierls, R., *Quantum Theory of Solids* (Clarendon, Oxford, 1955).

5. Cabot, M. and Putterman, S.J., Phys. Lett. **83A**, 91 (1981); Slonimski, G.L., Zh. Eksp. Theor. Fiz. **7**, 1457 (1937).

6. Zakharov, V.E., J. Appl. Mech. Tech. Phys. **6 (4)**, 22 (1965) [Russian original: Zh. Prikl. Mekh. Tekh. Fiz. **4**, 35]; Zakharov, V.E., *Basic Plasma Physics*, Vol. 2, edited by M.N. Rosenbluth and R.Z. Sagdeev (Elsevier, New York, 1984), Ch. 5.1, p. 3; Zakharov, V.E. and Sagdeev, R.Z., Sov. Phys. Dokl. **15**, 439 (1970); Kraichnan, R., Phys. Fluids **11**, 265 (1968); Sagdeev, R.Z., Rev. Mod. Phys. **51**, 1 (1979).

7. Kolmogorov, A.N., Dokl. Acad. Sci. URSS **30**, 301 (1941).

8. Larraza, A., Garret, S.L., Putterman, S., Phys. Rev. A **41**, 3144 (1990).

9. Larraza, A., *Universal power spectra for wave turbulence: Applications to Wind Waves, Flicker Noise, Solar Wind Spectrum, and Classical Second Sound*, Ph. D. Thesis, Dept. Phys. UCLA (1987).

10. Happek, U., Ayant, Y., Buisson, R., and Renk, K.F., Europhysics Letters, **3 (9)**, 1001 (1987); Happek, U., Baumgartner, R., and Renk, K.F., *Phonon Scattering in Condensed Matter*, edited by W. Eisenmenger, K. Labmann, and S. Dottinger (Springer, Berlin, 1984), p. 37.

11. Bron, W.E. and Grill, W., Phys. Rev. B **16**, 5303 (1977); Bron, W.E. and Grill, W., Phys. Rev. B **16**, 5315 (1977).

12. Putterman, S.J. and Roberts, P.H., Physics Reports **168**, 209 (1988).

13. Kazakovtsev, L. and Levinson, Y.B., Phys. Status Solidi B **96**, 117 (1979).

14. Musher, S.L., Phys. Lett. **70A**, No. 5, 361 (1979).

15. Zakharov, V.E. and Musher, S.L., Dokl. Akad. Nauk SSSR, **209**, No. 5, 1063 (1973).

FIGURE CAPTIONS

Figure 1. Time evolution of the classical wave turbulent spectrum from an initial Rayleigh-Jeans distribution with T=2000 to a steady-state spectral density that follows a -3/2 power law. An energy flux of 10^{24} is injected over a Gaussian distribution of modes centered around ω=3 and removed over a distribution of modes greater than 300.

Figure 2. Time evolution of the quantum wave turbulent spectrum from an initial Planck distribution with T=1.5 to a steady-state spectral density that follows a -6 power law. An energy flux of 1000 is injected over a Gaussian distribution of modes centered around ω=800 and removed over a Gaussian distribution of modes centered at ω=10.

Figure 3. Forward cascade of energy from the classical regime to the quantum regime for $q > q_c$. An energy flux = 10^{17} is input over a Gaussian distribution of modes centered at ω=3 and removed over modes greater than ω=300. The spectrum follows a -3/2 power law which then turns down with a slope steeper than Wien's law so as to meet the initial Planck distribution with T=35.

Figure 4. Forward cascade of energy from the classical regime to nonlinear quantum regime for $q \approx q_c$ and $q > q_c$. In plot A, $q = 6 \times 10^{19} \approx q_c$; in plot B, $q = 5 \times 10^{20} > q_c$. In both A and B an energy flux is input over a Gaussian distribution of modes centered at ω=4 and removed over modes greater than ω_p=280. Both curves follow a -3/2 power law before meeting the initial Planck spectrum with T=100.

Figure 5. Reverse Cascade of Energy from ω=560 to ω_p=28. An energy flux = 10^{13} is supplied over a Gaussian distribution of modes centered at ω=560 and similarly removed at ω_p=28. The spectrum initially follows a -6 power law before curving around to meet the initial Planck distribution with T=10.

FIGURE 1

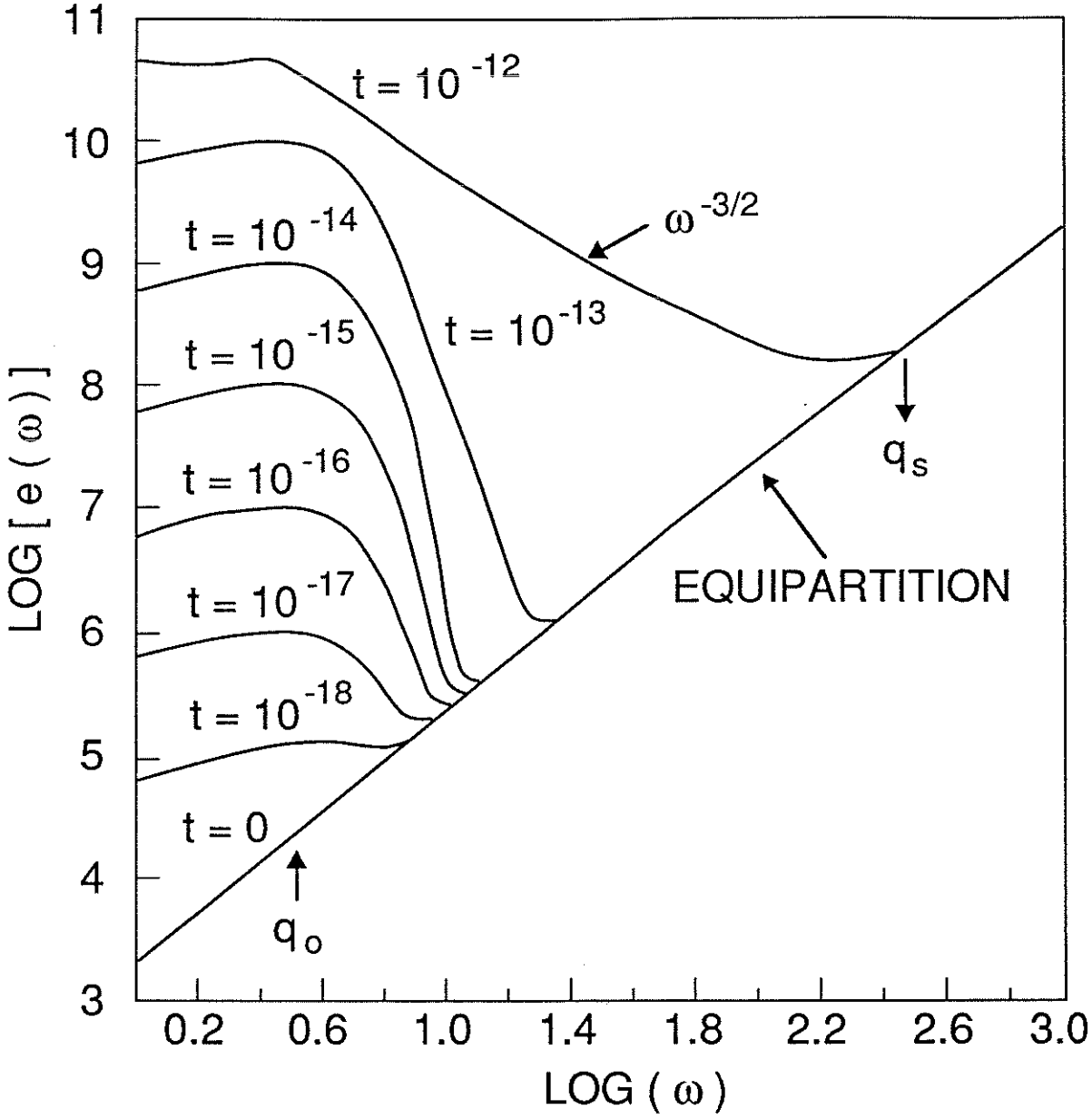
11
10
9
8
7
6
5
4
3
LOG [e (ω)]
0.2
0.6
1.0
1.4
1.8
2.2
2.6
3.0
LOG (ω)
t = 10 -12
t = 10 -14
t = 10 -15
t = 10 -16
t = 10 -17
t = 10 -18
t = 0
t = 10-13
ω -3/2
qs
EQUIPARTITION
qo

FIGURE 2

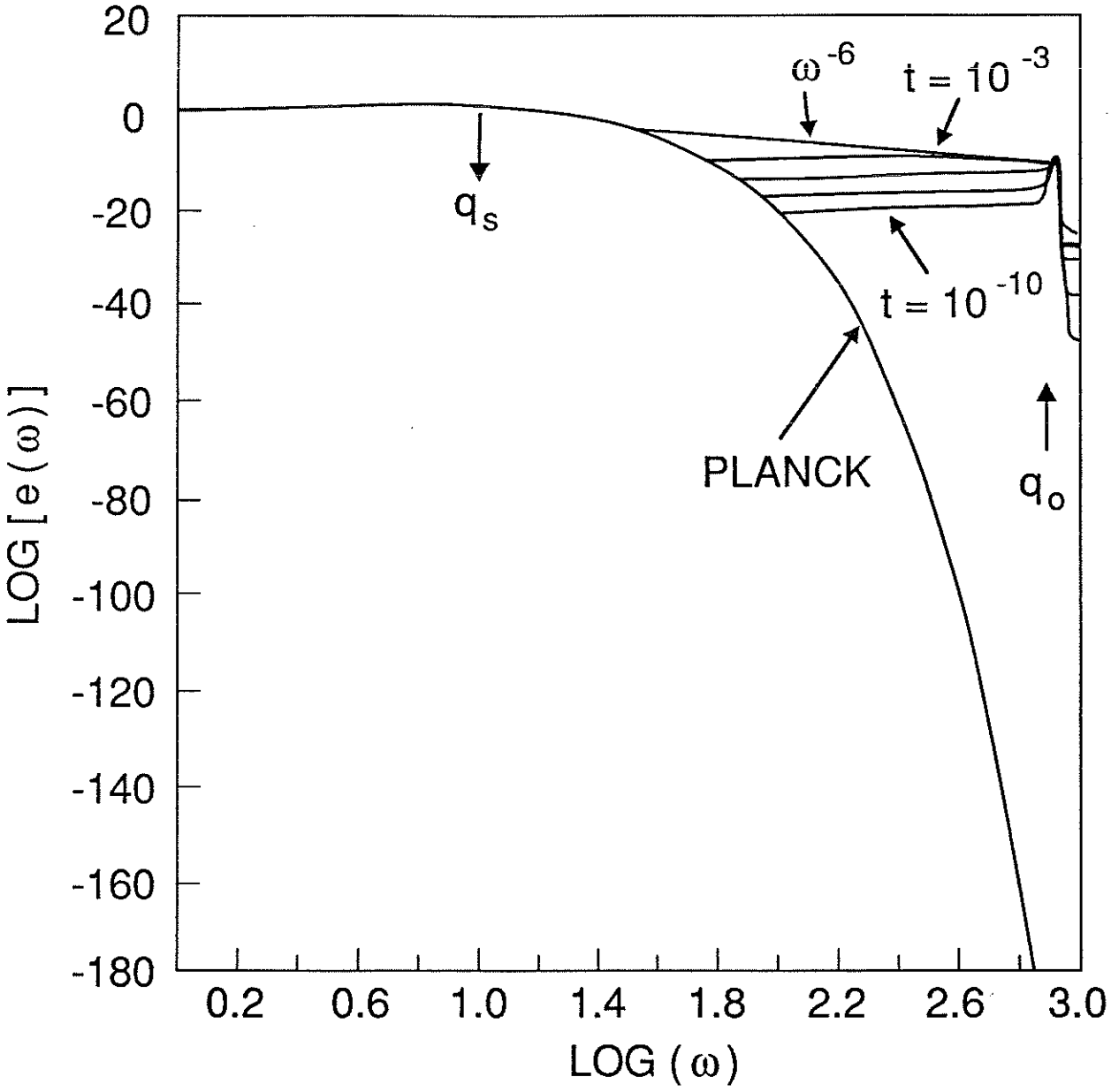
20
0
-20
-40
-60
-80
-100
-120
-140
-160
-180
LOG [e (ω)]
0.2
0.6
1.0
1.4
1.8
2.2
2.6
3.0
LOG (ω)
ω -6
t = 10 -3
t = 10 -10
q s
q o
PLANCK

FIGURE 3

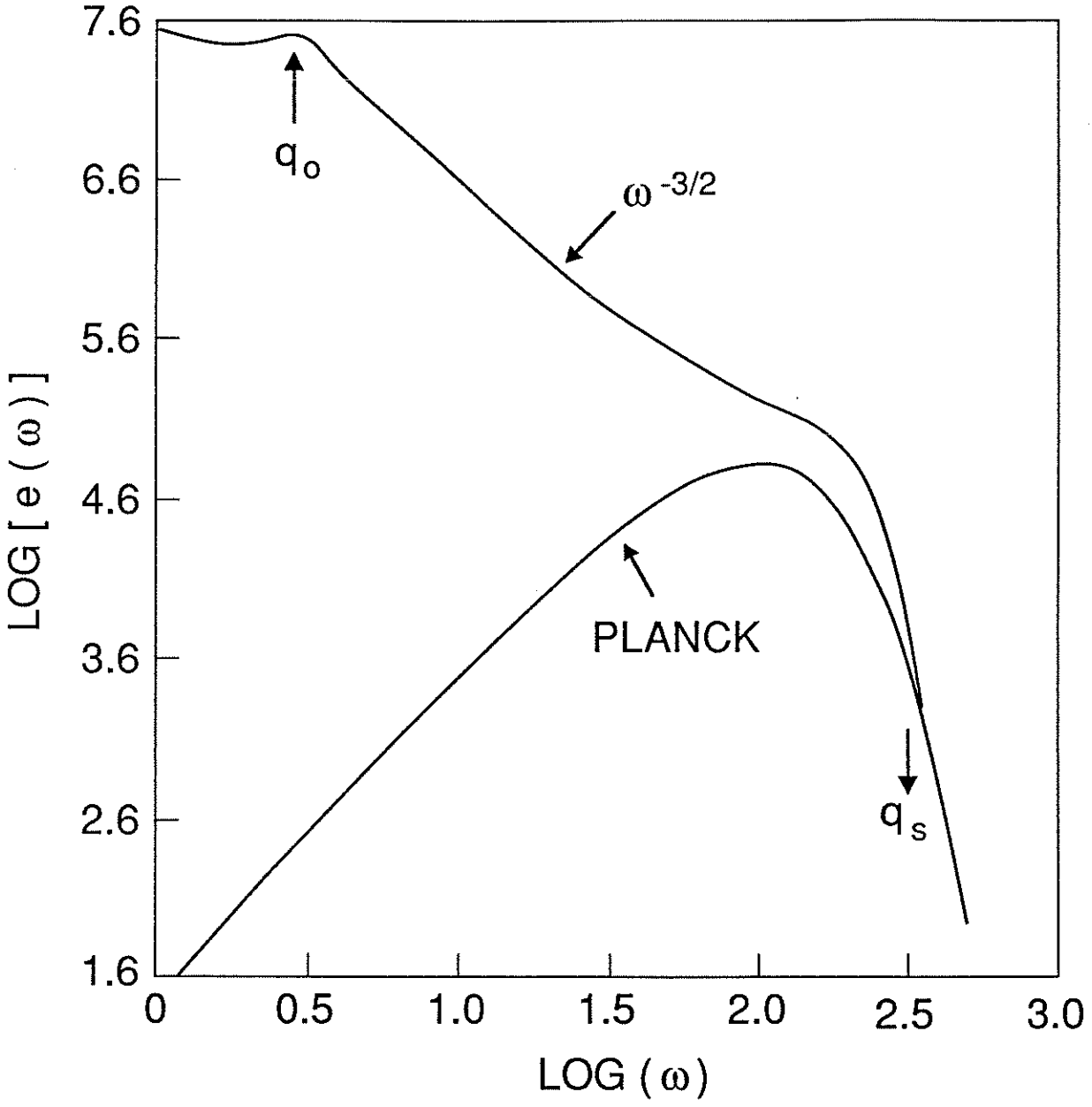
7.6
6.6
5.6
4.6
3.6
2.6
1.6
LOG [e (ω)]
0
0.5
1.0
1.5
2.0
2.5
3.0
LOG (ω)
q_o
$\omega^{-3/2}$
PLANCK
q_s

FIGURE 4

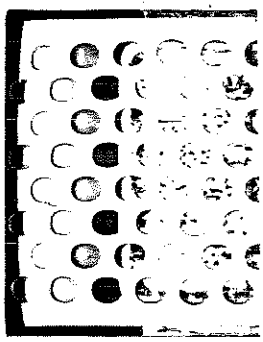

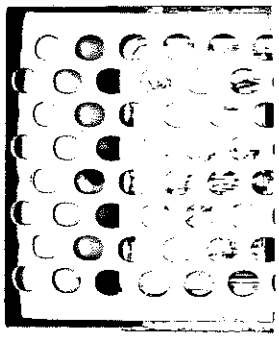

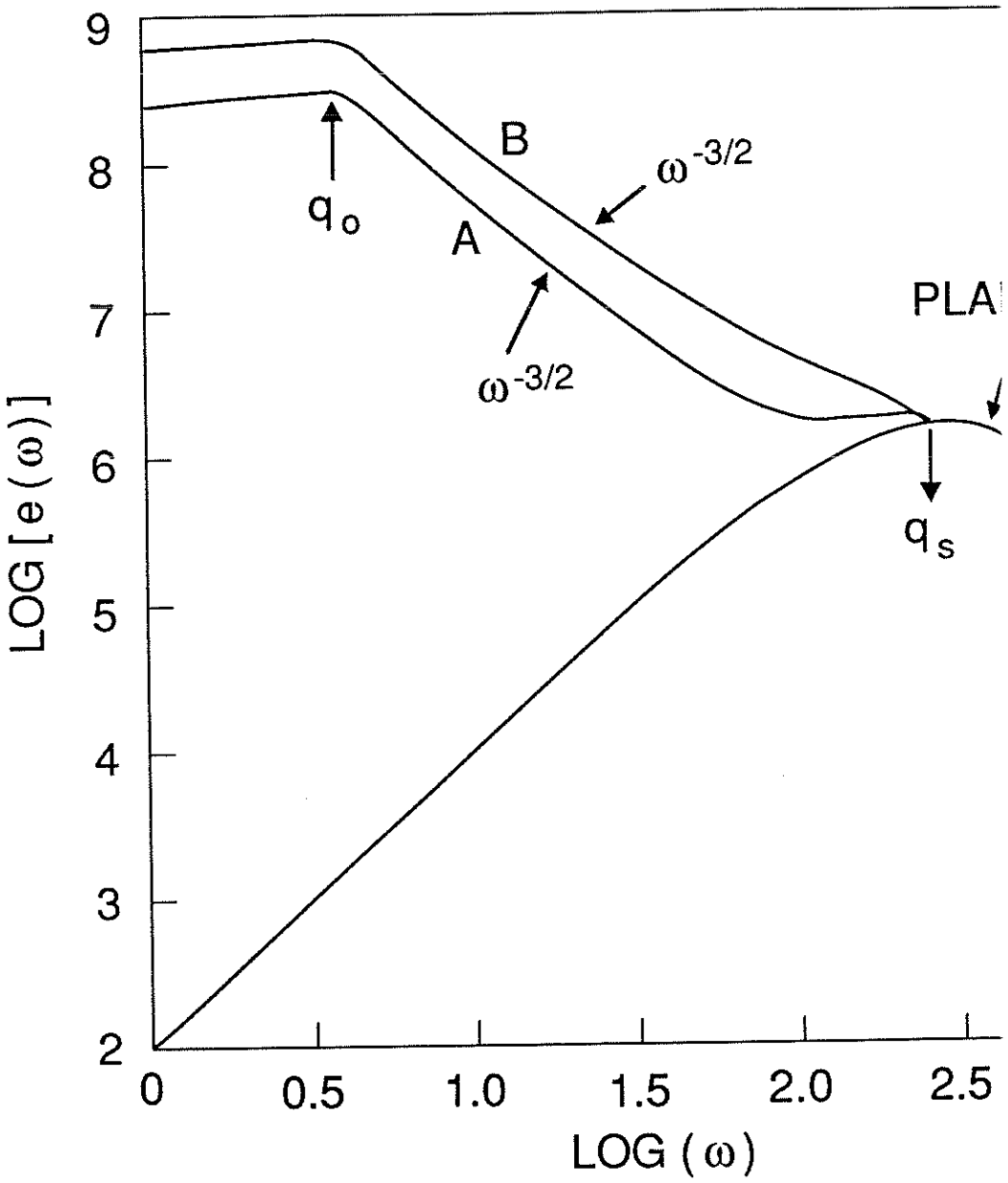
9
8
7
6
5
4
3
2
LOG [e (ω)]
0
0.5
1.0
1.5
2.0
2.5
LOG (ω)
B
A
$\omega^{-3/2}$
$\omega^{-3/2}$
q_o
q_s
PLA

FIGURE 5

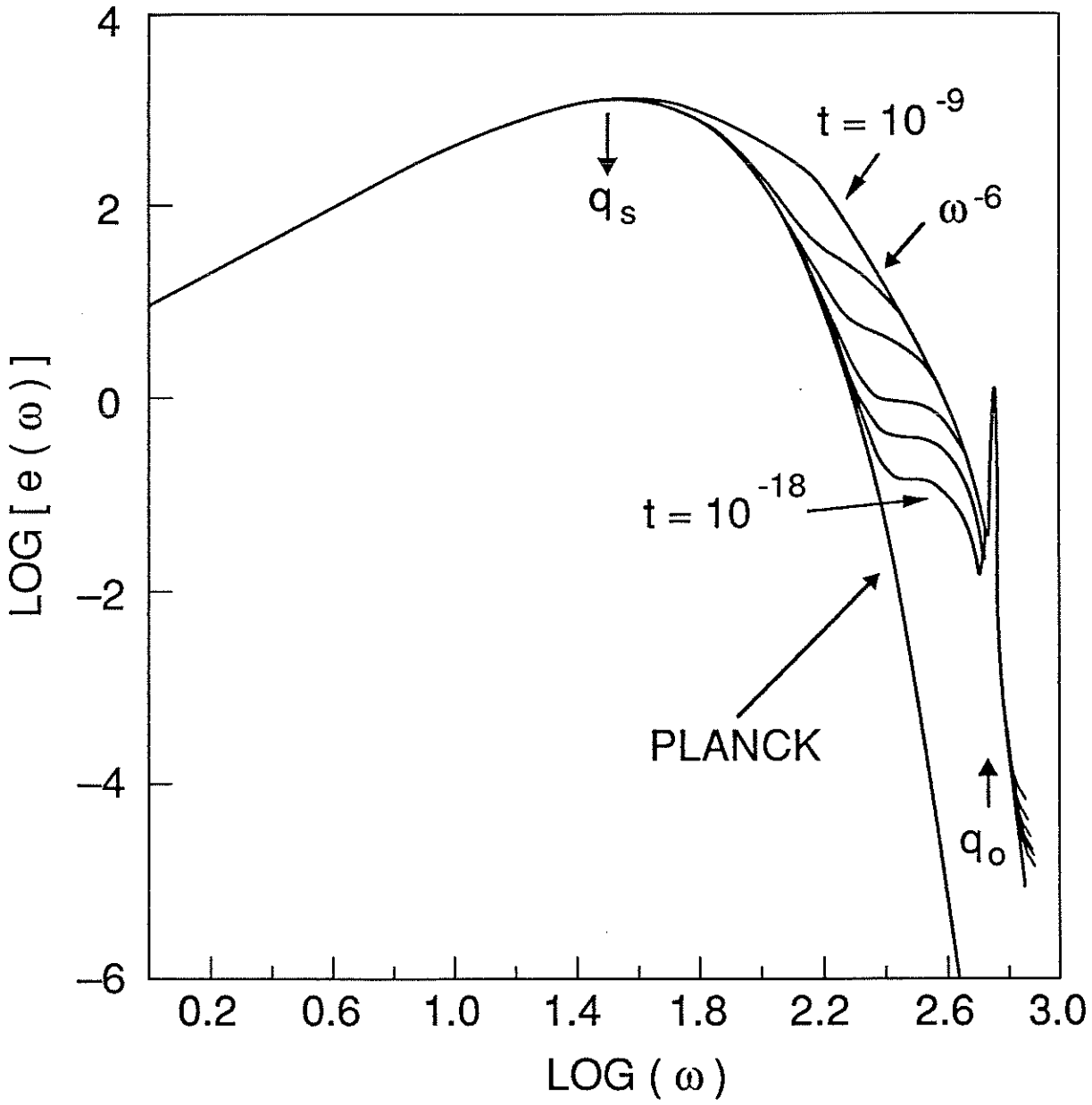
4
2
0
−2
−4
−6
LOG [e (ω)]
0.2
0.6
1.0
1.4
1.8
2.2
2.6
3.0
LOG (ω)
t = 10 -9
ω -6
q s
t = 10 -18
PLANCK
q o